Linear Stability Analysis of Rotating Spiral Waves in Excitable Media

Dwight Barkley

Program in Applied and Computational Mathematics, Princeton University, Princeton, New Jersey 08544

Fast numerical methods are used to solve the equations for periodically rotating spiral waves in excitable media, and the associated eigenvalue problem for the stability of these waves. Both equally and singly diffusive media are treated. Rotating-wave solutions are found to be discretely selected by the system and an isolated, complex-conjugate pair of eigenmodes is shown to cause instability of these waves. The instability arises at the point of *zero curvature* on the spiral interface and results in wavelike disturbances which propagate from this point along the interface.

Spiral waves are probably the most pervasive structures in nonequilibrium reaction-diffusion systems. These waves are observed in a wide range of contexts, from chemical reactions and physiological media to slime-mold aggregates and insect population dynamics [1]. While a general theoretical understanding of these spirals has been rapidly emerging through the efforts of several groups [2], the analytical treatment of spiral waves has proven extremely difficult, and as a result, there are still significant gaps in our understanding of the spirals so commonly observed in nonequilibrium media.

Of fundamental importance is the stability of a single, periodically rotating spiral wave in a two-dimensional excitable medium (Fig. 1). Such rotating spirals [3] are often observed to lose stability as some control parameter of the system is varied. This instability and the unsteady, i.e., quasiperiodic, spirals that ensue have been the subject of intense experimental and theoretical study [4–11]. Despite numerous investigations of this instability, very little is known definitively about its character other than that it typically arises via a Hopf bifurcation. Until now, there has been no direct linear stability analysis to determine explicitly the eigenvalues of rotating spirals or the form of the bifurcating eigenmodes. As we shall show, the bifurcating eigenmodes provide key insights into the

FIG. 1. Periodically rotating spiral wave in an excitable medium. The wave rotates counterclockwise at constant speed and is steady in the appropriately rotating frame. Contours of the fast variable u (equally spaced from $u=0.1$ to $u=0.9$) illustrate the sharp interface between the quiescent ($u=0$) and excited ($u=1$) states of the system. Parameters (listed in Fig. 2 caption) are such that the spiral wave is just at the instability to quasiperiodicity.

spatiotemporal character of the spiral instability. Moreover, the eigenvalue spectrum immediately determines whether the instability is associated with isolated or continuum of eigenvalues, and whether rotating spirals are themselves selected by the system. These basic issues for spiral waves are addressed here by employing fast numerical methods to solve the full, two-dimensional field equations for rotating spiral waves and the associated eigenvalue problem for the stability of these waves.

Our study is based on the two-species model of an excitable medium [7,12]:

$$\frac{\partial u}{\partial t} = \nabla^2 u + \epsilon^{-1} u (1-u) \left[u - \frac{v+b}{a} \right],$$

$$\frac{\partial v}{\partial t} = \delta \nabla^2 v + u - v,$$

(1)

where a, b, and ϵ are parameters of the reaction kinetics with $\epsilon \ll 1$, and δ is the ratio of diffusion coefficients. This model, like other two-variable models of this general type, faithfully captures the behavior of many excitable systems. Because of the smallness of ϵ, the u field takes on one of two states almost everywhere: quiescent ($u=0$) and excited ($u=1$). A thin interface, or reaction zone, separates the two regions (Fig. 1).

We seek rotating-wave solutions of (1), that is, solutions which satisfy $\partial_t = -\omega \partial_\theta$, where ω is the wave speed of the rotating wave. Such rotating waves satisfy the steady-state equation

$$0 = F(u) \equiv \delta \nabla^2 u + \omega \partial_\theta u + f(u),$$

(2)

where $u = (u,v)^T$, $\delta = \text{diag}(1,\delta)$, and $f(u)$ represents the kinetic terms in (1). The boundary conditions are $\partial_r u = 0$ on a circle of radius R, so that the system is rotationally symmetric. Equation (2) is a nonlinear eigenvalue problem for the wave speed ω.

Associated with (2) is the linear eigenvalue problem for the stability of rotating waves:

$$DF(u)\bar{u} = \lambda \bar{u},$$

(3)

where λ and $\bar{u}$ are the eigenvalues and eigenmodes of

field u, and

$$DF(u) = \delta \nabla^2 + \omega \partial_\theta + Df(u). \tag{4}$$

This linear eigenvalue problem is equivalent to the Floquet problem for rotating waves when viewed as a time-periodic orbit in the rest frame.

We solve (2) and (3) by representing all fields on a polar grid and solving the resulting discretized equations with numerical methods described fully elsewhere [13, 14]. Because the evolution equation for v in (1) is linear, v can be completely eliminated from the steady-state problem via a Green function. The remaining (nonlocal) steady-state problem is solved by Newton's method. This can be done in a fast way using Krylov methods [13] which exploit the fact that the right-hand side of (2) differs significantly from zero only in the vicinity of the thin u reaction zone. Because of rotational symmetry, solutions of (2) are determined only up to an arbitrary orientation in θ. This phase freedom is eliminated by augmenting (2) with an additional equation which pins the phase of the spiral. This extra equation allows ω to be treated as an additional unknown, thereby permitting the pair (u, ω) to be computed in concert. Newton iterations are started from a solution obtained by direct simulation of (1). Continuation is then used to obtain rotating-wave solutions at other parameter values, including parameters such that these solutions are unstable. The leading eigenvalues (those with largest real part) and their corresponding eigenmodes are obtained from (3) by direct application of the methods in [14].

For results reported in detail here, we have used $N_r = 121$ radial and $N_\theta = 256$ azimuthal grid points. The thin reaction zones in the u field are fully resolved. All operators are evaluated spectrally in the θ direction and using fourth-order finite differences in the r direction (except at $r = R$ where second order is used). Newton iterations of (2) are stopped when $||F(u)|| < 10^{-2}$; which is more than 100 times smaller than can reasonably be obtained by time stepping (1). Norms refer to the L_2 norm of the $2 \times N_r \times N_\theta$ discrete quantities. For eigenvalue problem (3), the residuals satisfy $||DF(u)\tilde{u} - \lambda \tilde{u}|| < 10^{-4}$.

Figure 2 shows the five leading eigenvalues for both the singly diffusive ($\delta = 0$) and equally diffusive ($\delta = 1$) cases. While our methods are applicable for any value of δ, we treat only these two cases here as they occur most frequently in practice. We find that as δ is varied from 0 to 1, the spiral instability shifts to smaller ϵ and larger a (for fixed b). Hence, in choosing the two representative examples to show in Fig. 2, it was necessary to vary the kinetic parameters accordingly. A survey of parameter space for this model will be presented elsewhere.

Consider first the eigenvalues on the imaginary axis. Because of rotational symmetry, rotating spiral waves have a zero eigenvalue, λ_R. As can be verified immediately from (3), the eigenmode with zero eigenvalue is
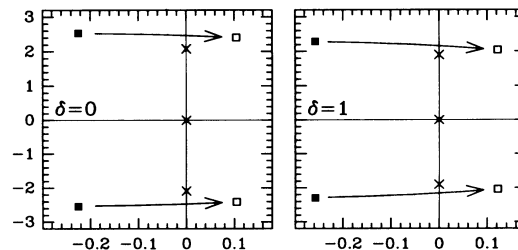
FIG. 2. Leading eigenvalue spectra for $\delta = 0$ and $\delta = 1$. Crosses show eigenvalues on the imaginary axis due to symmetries (or approximate symmetries) of the problem. Squares show bifurcating eigenvalues before and after the instability, with arrows indicating the path taken as they cross the imaginary axis. The bifurcation parameter is a. For $\delta = 0$ the parameter values are $a = 0.70$ (solid squares) and $a = 0.61$ (open squares), $b = 10^{-3}$, $\epsilon = 0.02$, and $R = 18$. For $\delta = 1$ the parameters are $a = 0.35$ (solid squares) and $a = 0.26$ (open squares), $b = 10^{-3}$, $\epsilon = 8 \times 10^{-3}$, and $R = 12$. Because of variation in wave speed with a, the purely imaginary eigenvalues vary slightly with a and are plotted at the bifurcation points: $a = 0.643$ ($\delta = 0$) and $a = 0.286$ ($\delta = 1$). The spiral in Fig. 1 is at the bifurcation point for $\delta = 0$.

$\tilde{u}_R = \partial_\theta u$, where u is the spiral solution of (2). For spirals on the infinite plane there is also translational symmetry, so that in a frame rotating with speed ω, there is a complex-conjugate pair of eigenmodes, $\tilde{u}_T = \partial_x u \pm i \partial_y u$, with eigenvalues $\lambda_T = \pm i\omega$. Translational symmetry is broken by our boundary conditions and we expect the eigenvalues to move slightly off the imaginary axis. However, for sufficiently large domains, the real part of these eigenvalues is numerically indistinguishable from zero. Specifically, over the range of parameters indicated in Fig. 2, we have the following numerical bounds for the eigenvalues on the imaginary axis. For $\delta = 0$, $|\lambda_R| < 3 \times 10^{-4}$, $|\mathrm{Re}(\lambda_T)| < 8 \times 10^{-4}$, and $|\mathrm{Im}(\lambda_T)/\omega - 1| < 5 \times 10^{-4}$. For $\delta = 1$, $|\lambda_R| < 4 \times 10^{-3}$, $|\mathrm{Re}(\lambda_T)| < 10^{-2}$, and $|\mathrm{Im}(\lambda_T)/\omega - 1| < 6 \times 10^{-3}$. These bounds testify to the accuracy of our numerical solutions.

Consider now the complex-conjugate pair of eigenvalues which cross the imaginary axis and lead to the spiral-wave instability (Hopf bifurcation). The method used to solve (3) necessarily produces eigenvalues ordered by their real part. Thus we know definitively that when the bifurcating eigenvalues λ_B are in the positive half plane, they are isolated: There are no other eigenvalues between (in the sense of real part) the bifurcating pair and those on the imaginary axis. In addition, we have tested the robustness of the bifurcating eigenvalues, both before and after the instability, to changes in grid resolution and domain radius R. In the case $\delta = 1$, $\mathrm{Re}(\lambda_B)$ varies under such changes by approximately the width of the squares plotted in Fig. 2; otherwise, the variation in λ_B is far less than the square size. We conclude that even for an infinite medium, the bifurcating eigenvalues are isolated, i.e., they lie in a discrete part of the spectrum of

operator (4). Hence, over a parameter range the spirals are unstable to a single pair of complex modes.

The spectra in Fig. 2 provide direct evidence that the spirals considered here are discretely selected by the system. This follows from the fact that the root of an equation is simple, hence isolated, if its linearization has no eigenvalues on the imaginary axis. Generically, there are no eigenvalues on the imaginary axes in Fig. 2 except those which can be accounted for from symmetry considerations. Hence, there are no spiral solutions near a pair (u,ω) except those obtained through symmetry operations and the spiral waves are not part of a continuum of solutions to (2) with continuously varying shape and/or wave speed [15].

The bifurcating eigenmode in the case $\delta = 0$ is detailed in Fig. 3. We focus on the u component of the eigenmode $\tilde{u}$. The eigenmode is localized at the thin interface of the spiral wave, and at the instability, it has an extremum exactly at the point of zero curvature along the $u = \frac{1}{2}$ contour of the spiral (see below). Hence we consider $\tilde{u}(s)$, where s is the arclength along this contour with $s \equiv 0$ at
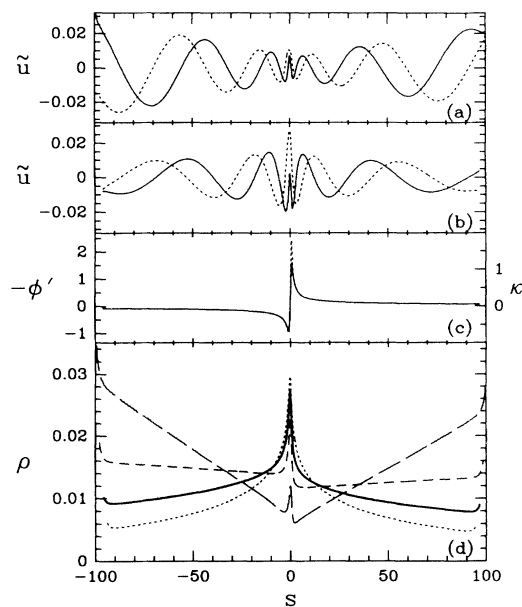
FIG. 3. Bifurcating eigenmode for the case $\delta = 0$. Parameters are as in Fig. 2. Results are plotted as a function of arclength s along the $u = \frac{1}{2}$ contour of the spiral wave, with $s \equiv 0$ at the point of zero curvature. (a) Real part, $\tilde{u}^r$ (solid curve), and negative imaginary part, $-\tilde{u}^i$ (dashed curve), of the bifurcating eigenmode prior to the bifurcation, $a = 0.70$. (b) Same as (a) except at the bifurcation, $a = 0.643$. (c) The eigenmode's local wave number, $-\phi'$ (solid curve), and curvature of the spiral wave, κ (dashed curve), at the bifurcation. The curves are indistinguishable except near the extrema. (d) Magnitude of the eigenmode, ρ, for several values of the parameter a. At the bifurcation, $a = 0.643$ (bold solid curve); before the bifurcation, $a = 0.70$ (long-dashed curve) and $a = 0.67$ (medium-dashed curve); after the bifurcation, $a = 0.61$ (short-dashed curve). Boundary effects are visible at the extremes of s.

the point of zero curvature $(\kappa = 0)$, and $s > 0$ on the leading edge of the spiral. The complex mode $\tilde{u}(s)$ is conveniently written as $\tilde{u}(s) = \tilde{u}^r(s) + i\tilde{u}^i(s)$ or as $\tilde{u}(s) = \rho(s)\exp[i\phi(s)]$.

Figures 3(a) and 3(b) show the real and imaginary parts of the bifurcating eigenmode prior to and at the instability. Eigenmode $\tilde{u}$ corresponds to a time-dependent perturbation of the form $\text{Re}[\tilde{u}\exp(\lambda_B t)]$, so that apart from the overall growth factor $\exp[\text{Re}(\lambda_B)t]$, $\tilde{u}^r(s)$ and $-\tilde{u}^i(s)$ illustrate the perturbation separated by $\Delta t = \pi/2\text{Im}(\lambda_B)$. Clearly the spiral instability corresponds to wavelike disturbances which propagate away from the point of zero curvature. This is shown quantitatively in Fig. 3(c) with a plot of curvature, $\kappa(s)$, for the bifurcating spiral and $-\phi'(s)$ for the critical eigenmode. $(-\phi' = -d\phi/ds$ is interpreted as the local wave number.) The local wave number of the eigenmode changes sign precisely at the point $\kappa = 0$, implicating this point as the source of counterpropagating waves. Everywhere except near the extrema in κ, $\phi' = -1.35\kappa$. Far from the tip, the data are consistent with the scaling: $\phi' \propto \kappa \sim 1/r$.

Further insight into the instability comes from the magnitude of the bifurcating eigenmode, $\rho(s)$, shown in Fig. 3(d). At the instability, $\rho(s)$ has a maximum exactly at the point of zero curvature and decays very slowly away from this point. The critical eigenmode is definitely not exponentially localized to the tip region; the numerical data are consistent with power-law decay $\rho(s) \sim |s|^{-\alpha}$, with $\alpha = 0.19 \pm 0.02$ at the instability. Because of the slowness of the decay, however, it is impossible to conclude with certainty its asymptotic form. The most surprising feature of the bifurcating eigenmode is its qualitative change just prior to the instability. Away from transition where the spiral is stable, $\rho(s)$ has a local maximum approximately at $s = 0$, but otherwise grows linearly along the spiral arm: $\rho(s) \sim |s|$. We have found this linear growth of the eigenmode generic for spirals far from the instability. Only very near the bifurcation does the extremum at $s = 0$ become dominant.

We find the bifurcating eigenmode for $\delta = 1$ to be qualitatively the same in all respects to the case $\delta = 0$ illustrated in Fig. 3. There is, however, significant quantitative variation with δ and we are unable to compute as many spiral wavelengths for the case $\delta = 1$. Figure 4 illustrates, with contour plots of the tip region, the critical eigenmodes for both $\delta = 0$ and $\delta = 1$. At this time we find no reason to believe that the two cases are fundamentally different as regards the spiral-wave instability.

The instability, as seen in the rotating frame, is summarized as follows. Just prior to the bifurcation, the destabilizing eigenmode develops a maximum at the point of *zero curvature* on the spiral interface. This point is then the center of the instability. After the instability sets in, periodic disturbances propagate away from this point in both directions along the interface. Both the amplitude and wave number of these disturbances decay slowly (i.e., power law) with distance from the tip region.
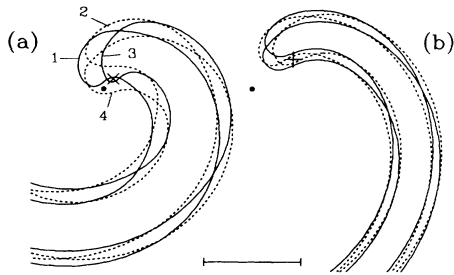
FIG. 4. Spirals perturbed by the real (solid lines) and imaginary (dashed lines) parts of the critical eigenmode. (a) $\delta=0$, $a=0.643$; (b) $\delta=1$, $a=0.286$. Contours are shown for the fields $u \pm \xi \bar{u}^r$ and $u \pm \xi \bar{u}^i$, where the constant ξ is chosen separately for (a) and (b) such that the contour envelope is approximately the interface width. The bar denotes 4 length units, circles denote grid centers, and crosses denote the points of zero curvature on the $u=\frac{1}{2}$ contours of the bifurcating spirals. Numbers in (a) indicate time ordering over one bifurcating period; contours in (b) have the same clockwise ordering. By observing contours at successive times, it is possible to discern the standing character of the eigenmodes at the crosses and their propagative character away from these points.

There are two caveats to the preceding picture. The first is that the contours of Fig. 4 have maximum amplitude variation, not at the point of zero curvature, but almost exactly at the point of maximum curvature. This is due to nonuniformity in the interface near the spiral tip (e.g., Fig. 1). At the present it is not known to what extent this nonuniformity persists as $\epsilon \to 0$. The parameters considered here are, nevertheless, appropriate for realistic systems. The second caveat is that for certain parameters the bifurcating eigenvalues coalesce with the imaginary pair due to translational symmetry. In the vicinity of such a coalescence, the bifurcating eigenmodes have the character of the translational modes. Such situations are, however, atypical.

As regards the *nonlinear* dynamics of Eqs. (1), direct simulations show that the bifurcations considered here are supercritical and saturate at finite amplitude. The fully nonlinear behavior in the vicinity of the bifurcations is similar to that reported previously for this [7,12] and other [4–6,8,11] models, and is in qualitative agreement with experimental studies of the spiral instability [5,9,10]. Further examination of the nonlinear behavior will be presented elsewhere.

In conclusion, we have elucidated key features of the spiral-wave stability problem through direct numerical solution of a model excitable medium. The model studied is representative of a broad class of excitable systems and we expect our results to be equally broad. Because we have obtained highly accurate solutions with no assumptions whatsoever as to their form, our results provide a valuable guide and benchmark for ongoing work using kinematic and free-boundary approaches to the study of spiral waves [2]. Contrary to what has been implicitly as-

sumed in the past, our results suggest that the spiral instability has little or nothing to do with the point of maximum curvature on the spiral interface. We have instead identified the point of zero curvature as the center of the instability and suggest that future studies focus on this point. Finally, when unsteady, i.e., quasiperiodic, spiral waves obtained from direct simulations are plotted in the rotating frame, the character of the destabilizing eigenmode is clearly seen. Hence, much of the eigenmode structure presented here should be visible in experimental data when viewed in the appropriately rotating frame.

[1] Four reviews containing numerous examples of spiral waves are the following: A. T. Winfree, *When Time Breaks Down* (Princeton Univ. Press, Princeton, 1987); V. S. Zykov, *Modelling of Wave Processes in Excitable Media* (Manchester Univ. Press, Manchester, 1988); J. J. Tyson and J. P. Keener, Physica (Amsterdam) **32D**, 327 (1988); **49D** (1991). Two other recent examples of spirals are S. Jakubith *et al.*, Phys. Rev. Lett. **65**, 3013 (1990); M. P. Hassel, H. N. Comins, and R. M. May, Nature (London) **353**, 225 (1991).

[2] Tyson and Keener (Ref. [1]) provide an excellent review. Recent work includes P. Pelcé and J. Sun, Physica (Amsterdam) **48D**, 353 (1991); E. Meron, Physica (Amsterdam) **49D**, 98 (1991); A. S. Mikhailov and V. S. Zykov, Physica (Amsterdam) **52D**, 379 (1991); A. J. Bernoff, Physica (Amsterdam) **53D**, 125 (1991); A. Karma, Phys. Rev. Lett. **68**, 397 (1992); D. A. Kessler, H. Levine, and W. N. Reynolds, Phys. Rev. Lett. **68**, 401 (1992); J. P. Keener, SIAM J. Appl. Math. (to be published).

[3] By rotating spiral, we shall always mean periodically rotating wave, i.e., a rotating wave in the strict sense, D. A. Rand, Arch. Rat. Mech. Anal. **79**, 1 (1982).

[4] V. S. Zykov, Biofizika **31**, 862 (1986).

[5] W. Jahnke, W. E. Skaggs, and A. T. Winfree, J. Phys. Chem. **93**, 740 (1989).

[6] E. Lugosi, Physica (Amsterdam) **40D**, 331 (1989).

[7] D. Barkley, M. Kness, and L. S. Tuckerman, Phys. Rev. A **42**, 2489 (1990).

[8] A. Karma, Phys. Rev. Lett. **65**, 2824 (1990).

[9] T. Plesser, S. C. Müller, and B. Hess, J. Phys. Chem. **94**, 7501 (1990).

[10] G. S. Skinner and H. L. Swinney, Physica (Amsterdam) **48D**, 1 (1991).

[11] A. T. Winfree, Chaos **1**, 303 (1991).

[12] D. Barkley, Physica (Amsterdam) **49D**, 61 (1991).

[13] Y. Saad and M. H. Schultz, SIAM J. Sci. Stat. Comp. **7**, 856 (1986); W. S. Edwards, L. S. Tuckerman, R. A. Friesner, and D. C. Sorensen (to be published); D. Barkley (to be published).

[14] I. Goldhirsch, S. A. Orszag, and B. K. Maulik, J. Sci. Comp. **2**, 33 (1987).

[15] This selection of spiral waves is not unexpected, see, e.g., [2] and Tyson and Keener in [1].